Proceedings of the ASME 2016 International Design Engineering Technical Conferences & Computers and Information in Engineering Conference
IDETC/CIE 2016
August 21 – August 24, 2016, Charlotte, NC, USA

DETC2016-59408

TOPOLOGY OPTIMIZATION UNDER LINEAR THERMO-ELASTIC BUCKLING

Shiguang Deng, Krishnan Suresh

ksuresh@wisc.edu

UW-Madison, Madison, Wisconsin 53706, USA

ABSTRACT*

This paper focuses on topology optimization of structures subject to a compressive load in a thermal environment. Such problems are important, for example, in aerospace, where structures are prone to thermally induced buckling.

Popular strategies for thermo-elastic topology optimization include Solid Isotropic Material with Penalization (SIMP) and Rational Approximation of Material Properties (RAMP). However, since both methods fundamentally rely on material parameterization, they are often challenged by: (1) pseudo buckling modes in low-density regions, and (2) ill-conditioned stiffness matrices.

To overcome these, we consider here an alternate level-set approach that relies discrete topological sensitivity. Buckling sensitivity analysis is carried out via direct and adjoint formulations. Augmented Lagrangian method is then used to solve a buckling constrained compliance minimization problem. Finally, 3D numerical experiments illustrate the efficiency of the proposed method.

1. INTRODUCTION

Topology optimization has rapidly evolved from an academic exercise into an exciting discipline with numerous industrial applications [1], [2]. Applications include optimization of aircraft components [3], [4], spacecraft modules [5], automobiles components [6], cast components [7], compliant mechanisms [8]–[11], etc.

The focus of this paper is on thermo-elastic buckling topology optimization where structures are restrained and subject to thermal loading. For example, consider the wing rib structure of a high Mach supersonic aircraft in Figure 1. During rocket boost phase when the aircraft is subject to rapid acceleration and significant thermal gradients, its surface temperature can be as high as $1650^0 C$. Since the rib structures are welded onto wing skins, uneven thermal heating may induce significant compressive stresses to cause buckling. Therefore, a primary goal for structural designs of airplanes operating in extreme thermal environment is to provide a light-weight structure with thermal buckling resistance.

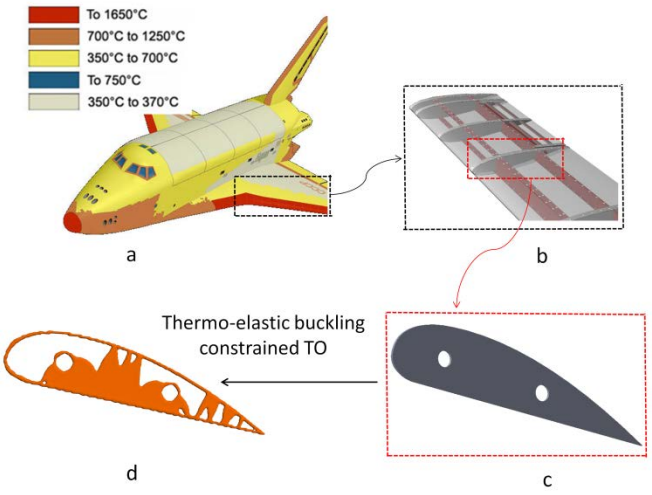

Figure 1: (a) aircraft operating in high temperature [www.buran-energia.com]; (b) wing rib structures [www.ae.metu.edu.tr]; (c) design space of rib structure; (d) optimized rib structure.

However, unlike in pure elasticity, for thermo-elastic problems, the displacements are computed after accounting for the additional thermal load. This poses both theoretical and computational challenges in topology optimization discussed later in the paper.

In Section 2, popular methods for buckling topology optimization are reviewed. Some of the challenges that remain are identified. In Section 3, we provide a brief of necessary technical background followed by proposed method and its implementation. In Section 4, numerical experiments are presented, followed by conclusions in Section 5.

2. LITERATURE REVIEW

2.1 Buckling constrained topology optimization

Buckling problems mostly occur in thin-walled structures [12]. Buckling constrained topology optimization problems were originally studied by ground structure method, while more recent methods are continuum based and can be classified into the following types: Solid Isotropic Material with Penalization (SIMP), evolutionary structural optimization (ESO) and level-set. In following sections, we review previous publications based on their methods.

Ground structure approach

Ground structure approach is the classic method for optimizing the topology of truss systems. In this approach, a network of potential truss members is first prescribed in a design domain. A size optimization is carried out on each truss member until the cross-section areas of non-optimal trusses approach zero and can therefore be removed [13].

However, including buckling constraint into truss topology optimization is non-trivial. The member forces in each truss have to satisfy functions which discontinuously depend on design variables [14]. Traditional optimizers face difficulty in solving such problems. In [14], the author argued that including slenderness constraints into buckling problems can guarantee solution existence and simplify the process. In [15], by using a smooth procedure to remove singular optimum from original formulation, size optimization was made more efficient. In a recent publication [16], the author used a mixed variable formulation to linearize buckling constraints in each ground structure member.

Solid Isotropic Material with Penalization (SIMP)

In the discipline of continuum structural topology optimization, the most popular method is SIMP. Its primary advantages are that it is well understood, robust and easy to implement [17]. Indeed, SIMP has been applied to a variety of topology optimization problems ranging from fluids to non-linear structural mechanics.

However, the 'singularity-problem' associated with zero-density elements require careful treatment, for example through epsilon-methods [18], [19]. Secondly, the ill-conditioning of the stiffness matrices, due to low-density elements, can lead to high computational costs for iterative solvers [20], [21].

The challenge of SIMP in buckling constrained topology optimization problem is the appearance of pseudo buckling modes in low-density regions. In [22], a buckling load criterion was introduced to ignore the geometric stiffness matrix of the elements whose density and principal stress were smaller than a prescribed value. In [23], the author argued such cut-off method may abruptly change objective function and sensitivity field, which often leaded to oscillating solutions. Instead, the author suggested using different penalization scheme for stiffness matrix and geometric stiffness matrix. Although the author in [24] suggested it was difficult to select a appropriate penalty scheme for accurate calculation of buckling load factor, the proposed approach by [23] became a popular formulation for many researchers [25]. In a recent publication [26], a new approach to remove pseudo buckling mode was based on eigen-value shift, and pseudo mode identification.

ESO

ESO [27] is an alternate topology optimization formulation where finite elements are gradually removed based on their significant levels to objective function. BESO [28] addresses some of the limitations of ESO by permitting insertion of elements.

In [29], a modified ESO method was proposed to maximize linear buckling load factor. The sensitivity number of the lowest eigen-value was first derived. The buckling eigen-value maximization was then formulated by appropriately selecting optimum criteria, based on the previously calculated sensitivity.

Level-Set

The level-set strategy is gaining popularity for solving topology optimization problems for several reasons: the boundary is well-defined at all times, the stress-singularity problem does not arise, and the stiffness matrices are typically well-conditioned; see [30] for a recent review and comparison of level-set based methods in structural topology optimization.

In [31], a simplified buckling sensitivity field was incorporated into a level-set based framework to accelerate large-scale topology optimization process.

2.2 Proposed method

Research gap

From the above literature review, one can conclude that there have been significant research devoted to solving buckling constrained topology optimization problems. However, one can identify the following research gaps:

- Although thermal buckling is of significant importance to stability analysis of structures under thermal gradients, there is very little research on buckling constrained thermo-elastic topology optimization.
- Computing buckling topological sensitivity is expensive, and efficient approaches are needed.

Proposed

In this paper, we adopt a level-set method due to its inherent advantages. However, instead of relying on the Hamilton-Jacobi equations for level-set propagation [32], we rely on fixed-point iteration to advance the topology [21]. Therefore, the domain need not be initialized with holes. The thermo-elastic buckling topological sensitivity field is calculated through two distinct approaches: direct and adjoint methods. The two approaches are tested and compared on 3D large-scale models.

3. PROBLEM FORMULATION AND ALGORITHM

3.1 Optimization problem formulation

Topology optimization of continuum structures often results in designs with column and thin-walled structures. External thermal gradients may introduce compressive stress in such structural components, causing buckling. Thus, by accounting for the buckling constraint, a thermo-elastic compliance minimization topology optimization problem can be posed as:

$$\begin{aligned} &\underset{\Omega\subset\Psi}{Min}\left|\Omega\right| \\ &J \le \alpha_1 J_0 \\ &P \ge \alpha_2 P_0 \\ &\text{subject to} \\ &K_t t = q \\ &Kd = f = f_m + f_{th} \end{aligned} \tag{1}$$

where:

Ω : Topology to be computed

Ψ : Design domain

t : Temperature field

d : Displacement field

K_t : Thermal stiffness matrix

K : Structural stiffness matrix

q : Heat flux

f : Total external load

f_{st} : Mechanical load

f_{th} : Thermal load

J : Compliance

J_0 : Initial compliance

P : Buckling load factor

P_0 : Initial buckling load factor

In words, the objective is to find the optimal topology with minimal volume within the design domain (Ψ) while satisfying prescribed compliance and buckling constraints. During the optimization process, the displacement and temperature fields are calculated from thermo-elastic finite element analysis discussed below.

3.2 Thermo-elastic finite element analysis

Finite element formulations of (weakly-coupled) thermo-elastic problems essentially reduce to solving two linear equations:

$$K_t t = q \tag{2}$$

$$Kd = f = f_{st} + f_{th} \tag{3}$$

The elemental thermal load vector in Equation (3) is formed via [33]:

$$f_e^{th} = \int_{\Omega_e} B^T D \varepsilon_e^{th} d\Omega \tag{4}$$

$$\varepsilon_e^{th} = \alpha(t_e - t_0)\Phi^T \tag{5}$$

where:

f_e^{th} : Element thermal load vector

Ω_e : Element domain

B : Element strain-displacement matrix

D : Element elasticity matrix

ε_e^{th} : Element thermal strain vector

α : Thermal expansion coefficient

t_e : Element temperature

t_0 : Reference temperature

Φ : [1 1 1 0 0 0] in 3D; [1 1 0] in 2D

The stresses are obtained by subtracting the thermal strain from the total strain, and multiplying the resulting strain by the material tensor:

$$\sigma_e = DBd_e - D\varepsilon_e^{th} \tag{6}$$

Further explanations and details may be found, for example, in [34]. The compliance for a thermo-elastic system is defined as:

$$J = (f + f^{th})^T d = d^T K d \tag{7}$$

It is noted in this paper the temperature within the design domain is increased uniformly, so that solving Equation (2) is unnecessary. Also, observe that Equation (3) represents a weakly-coupled problem where the thermal field influences the displacements, but not the inverse. Strongly-coupled thermo-elastic problems are beyond the scope of this paper.

3.3 Buckling sensitivity analysis

In this section, two approaches are used to calculate the sensitivity of linear buckling load factor. The linear buckling load factor can be calculated from a well-known formulation [12]:

$$(K + \lambda K_\sigma)\upsilon = 0 \tag{8}$$

where

K_σ : Global geometric stiffness matrix

λ : Linear buckling load factor

υ : Buckling mode vector

In Equation (8), the global geometric stiffness matrix is defined via the assembly:

$$K_\sigma = \sum_{e=1}^{N} [\mathrm{k}_\sigma]_e \tag{9}$$

where N is the number of finite elements and the elemental geometric stiffness matrix are defined as:

$$[\mathrm{k}_\sigma]_e = \int_{\Omega_e} G^T S G dv \tag{10}$$

where G is obtained from shape functions by appropriate differentiation and reordering [12]. The matrix S can be defined as:

$$\mathrm{S} = \begin{bmatrix} s & 0 & 0 \\ 0 & s & 0 \\ 0 & 0 & s \end{bmatrix} \tag{11}$$

where

$$s = \begin{bmatrix} \sigma_x & \tau_{xy} & \tau_{xz} \\ \tau_{xy} & \sigma_y & \tau_{yz} \\ \tau_{xz} & \tau_{yz} & \sigma_z \end{bmatrix} \tag{12}$$

In addition, the stress in an element can be defined as:

$$[\sigma]_e = [\sigma_x, \sigma_y, \sigma_z, \tau_{xy}, \tau_{xz}, \tau_{yz}]^T \tag{13}$$

It is clear that in Equation (8) the geometric stiffness matrix K_σ is a function of stress (σ) which depends on the topological design variable, while the stiffness matrix (K), buckling load factor (λ) and buckling mode vector (υ) are explicitly dependent on design variables. It is also noted since the temperature field is uniformly elevated to a prescribed value, the temperature field (t) is not dependent on those quantities.

Let Q be any quantity of interest in an optimization problem. The sensitivity of Q with respect to any design variable is defined as:

$$Q' = \frac{\partial Q}{\partial x} \tag{14}$$

The derivatives of the global stiffness matrix and geometric stiffness matrix can be expressed as:

$$K' \equiv \frac{\partial K}{\partial x} \tag{15}$$

$$K_\sigma{}' \equiv \frac{\partial K_\sigma}{\partial \sigma}\sigma' \tag{16}$$

Direct method

Multiplying the buckling mode vector (υ^T) on both sides of Equation (8), and taking the derivative with respect to design variable, we have:

$$2\upsilon'^T(K + \lambda K_\sigma)\upsilon + \upsilon^T(K' + \lambda K_\sigma{}' + \lambda' K_\sigma)\upsilon = 0 \tag{17}$$

Due to Equation (8), the first term in Equation (17) vanishes. Reordering terms in Equation (17), we have the sensitivity of the linear buckling load factor as:

$$\lambda' = -\frac{\upsilon^T(K' + \lambda K_\sigma{}')\upsilon}{\upsilon^T K_\sigma \upsilon} \tag{18}$$

A simple method to calculate ($K_\sigma{}'$) is to use finite difference, i..e, calculate the effect of removing a single element on the global geometric stiffness matrix. Obviously, this method is too expensive for topology optimization … the computational cost will increase significantly with the number of elements. Alternatively, we can employ a more direct and efficient approach.

The term on the right hand side of Equation (16) can be written as the summation of all finite elements:

$$\frac{\partial K_\sigma}{\partial \sigma}\sigma' = \sum_{j=1}^{N}\left(\frac{\partial K_\sigma}{\partial \sigma_j}\sigma_j'\right) \tag{19}$$

where N is the number of all finite elements. In words, the sensitivity of global geometric stiffness matrix equals the summation of the combinational effect between sensitivity of global geometric stiffness matrix with respect to each finite element stress and the sensitivity of the elemental stress.
For a specific j-element in Equation (19), reuse the summation rule as Equation (19):

$$\frac{\partial K_\sigma}{\partial \sigma_j}\sigma_j{}' = \sum_{k=1}^{6}\left(\frac{\partial K_\sigma}{\partial \sigma_{jk}}\sigma_{jk}'\right) \tag{20}$$

where the summation refers to the six elemental stress components in Equation (13). Further:

$$\frac{\partial K_\sigma}{\partial \sigma_{jk}} = \frac{\partial \int_{\Omega_j} G^T S G dv + \sum_{i=0}^{others}\left(\int_{\Omega_i} G^T S G dv\right)}{\partial \sigma_{jk}} \tag{21}$$

Since the geometric stiffness matrices in other elements are not explicitly dependent on the stress in j-element (σ_j^k), the second term in numerator of Equation (21) can be dropped:

$$\frac{\partial K_\sigma}{\partial \sigma_j^k} = \frac{\partial \int_{\Omega_j} G^T S G dv}{\partial \sigma_j^k} = \int_{\Omega_j} G^T \frac{\partial S}{\partial \sigma_k} G dv \tag{22}$$

where

$$\frac{\partial S}{\partial \sigma_k} = \begin{bmatrix} \frac{\partial s}{\partial \sigma_k} & 0 & 0 \\ 0 & \frac{\partial s}{\partial \sigma_k} & 0 \\ 0 & 0 & \frac{\partial s}{\partial \sigma_k} \end{bmatrix} \tag{23}$$

For the six stress components in Equation (13), it is easy to calculate their matrices elements in Equation (23). For example, when $k = 1$, we have:

$$\frac{\partial s}{\partial \sigma_1} = \begin{bmatrix} 1 & 0 & 0 \\ 0 & 0 & 0 \\ 0 & 0 & 0 \end{bmatrix} \tag{24}$$

The term ($\frac{\partial \sigma_j^k}{\partial x}$) in Equation (20) can be derived as follows. Rewrite Equation (6) for the j-element:

$$\sigma_j = DBd_j - D\varepsilon_j^{th} \tag{25}$$

where the elemental thermal strain (ε_j^{th}) can be calculated in Equation (5). Clearly, it is independent of design variable (x). Take derivative of each term in Equation (25), we have:

$$\sigma_j' = DBd_j + DBd_j' \tag{26}$$

We can calculate the term (d_j') in Equation (26) in the following manner. Taking derivative of the static equilibrium equation in Equation (3):

$$K'd + Kd' = f_{th}{}' \tag{27}$$

where the structural force is assumed independent of design variable. Reordering terms, we have

$$d' = K^{-1}(f_{th}{}' - K'd) \tag{28}$$

The elemental displacement sensitivity in j-element (d_j') can be directly obtained from Equation (28).

Adjoint method

An efficient way to compute the sensitivity field of buckling load factor is by adding adjoint variables and constraints into Equation (8) [35]. By carefully selecting the adjoint variables, the computational expensive terms ($\sigma_j{}'$) and ($d_j{}'$) in Equation (26) and (28) are expected to drop.

Multiplying buckling mode vector (υ^T) on both sides of Equation (8) and augmenting with two constraints multiplied by two adjoint variables (μ) and (w), we have:

$$\upsilon^T(K + \lambda K_\sigma)\upsilon + \mu^T[\sigma - Yd + Z\varepsilon_{th})] + w^T(f - Kd) = 0 \tag{29}$$

where the matrix (Y) and (Z) relate displacement and thermal strain to stress, respectively.

$$Y = \sum_{j=1}^{N}[\mathrm{DB}]_j \tag{30}$$

$$Z = \sum_{j=1}^{N}[\mathrm{D}]_j \tag{31}$$

In Equation (29), the adjoint μ link the stress to deformation, and the adjoint w link the deformation to external load. Then, taking derivative of Equation (29) and simplifying terms, we get:

$$\upsilon^T(K'+\lambda\frac{\partial K_\sigma}{\partial\sigma}\sigma'+\lambda' K_\sigma)\upsilon+\mu^T(\sigma'-Y'd-Yd'+Z'\varepsilon_{th})+ \\ w^T(f'-K'd-Kd')=0 \tag{32}$$

The first adjoint (μ) is chosen such that the terms with (σ') can be dropped from Equation (32):

$$\lambda v^T\frac{\partial K_\sigma}{\partial\sigma}\sigma'v+\mu^T\sigma'=0 \tag{33}$$

After factoring and rearranging terms, we have:

$$\mu^T=-\lambda v^T\frac{\partial K_\sigma}{\partial\sigma}v \tag{34}$$

where the term $\frac{\partial K_\sigma}{\partial\sigma}$ is the assembly of all elemental sensitivities, each containing six components.

$$\frac{\partial K_\sigma}{\partial\sigma}=\sum_{j=1}^{N}\sum_{k=1}^{6}\frac{\partial K_\sigma}{\partial\sigma_j^k} \tag{35}$$

where the term $\frac{\partial K_\sigma}{\partial\sigma_j^k}$ can be calculated from Equation (22).

Equation (32) simplifies to:

$$\upsilon^T(K'+\lambda' K_\sigma)\upsilon+\mu^T(-Y'd-Yd'+Z'\varepsilon_{th})+ \\ w^T(f'-K'd-Kd')=0 \tag{36}$$

The second adjoint w is chosen such that the terms containing d' can be cancelled out:

$$\mu^T Yd'+w^T Kd'=0 \tag{37}$$

After rearranging terms, we have:

$$w^T=-\mu^T YK^{-1} \tag{38}$$

Therefore, the sensitivity of the buckling load factor can be expressed as:

$$\lambda'=-\frac{1}{\upsilon^T K_\sigma\upsilon}(\upsilon^T K'\upsilon+\mu^T Z'\varepsilon_{th}-\mu^T Y'd+w^T f'-w^T K'd) \tag{39}$$

3.4 Discrete element sensitivity approximation

The last step is to compute the sensitivity of the global matrices in Equation (18) and (39), i.e., K', K_σ^x, Y' and Z'. If pseudo-density parameterization is used (e.g. SIMP), then the sensitivities can be computed via their respective material interpolation scheme [36]. One of the challenges with this approach is that the stiffness matrices will exhibit large condition numbers due to the elements with intermediate densities [37]. This will result in slow convergence of iterative solvers.

Here, we employ a discrete approximation, i.e., the sensitivities of the stiffness matrices are computed at the center of each element [38], i.e.:

$$K'\equiv\left[K_e\right] \tag{40}$$

$$Y'\equiv\left[DB\right] \tag{41}$$

$$Z'\equiv\left[D\right] \tag{42}$$

and then smoothened.

3.5 Augmented Lagrangian method

In order to solve the thermo-elastic TO problem posed earlier in Equation (1). The constraints can be absorbed into the objective function through the augmented Lagrangian [39]:

$$L(x,d,\Omega;\gamma_i,\mu_i)\equiv\varphi+\sum_{i=1}^{m}\overline{L}_i(x,d,\Omega;\gamma_i,\mu_i) \tag{43}$$

where

$$\overline{L}_i(x,d,\Omega;\gamma_i,\mu_i)=\begin{cases}\mu_i g_i+\frac{1}{2}\gamma_i(g_i)^2 & \mu_i+\gamma_i g_i>0\\ \frac{1}{2}\mu_i{}^2/\gamma_i & \mu_i+\gamma_i g_i\le 0\end{cases} \tag{44}$$

where

$$\begin{aligned}&L:\text{ Augmented Lagrangian}\\ &\overline{L}_i:\text{ Auxiliary Lagrangian}\\ &\mu_i:\text{ Lagrangian multipliers}\\ &\gamma_i:\text{ Penalty parameters}\\ &m:\text{ Number of constraints}\end{aligned} \tag{45}$$

Observe that the gradient of augmented Lagrangian with respect to design variable (x) is given by:

$$L'=\varphi'+\sum_{i=1}^{m}\overline{L}_i' \tag{46}$$

where

$$\overline{L}_i'=\begin{cases}\left(\mu_i+\gamma_i g_i\right)g_i' & \mu_i+\gamma_i g_i>0\\ 0 & \mu_i+\gamma_i g_i\le 0\end{cases} \tag{47}$$

The buckling sensitivity can be computed by Equation (18) and (39) while the sensitivity of compliance can be found in [38].

The Lagrangian multipliers and penalty parameters are initialized to an arbitrary set of positive values. Then the augmented Lagrangian is minimized using, for example, conjugate gradient method. In every iteration, the Lagrangian multipliers are updated as follows:

$$\mu_i^{k+1}=\max\{\mu_i^k+\gamma_i g_i(\hat{x}^k),0\},i=1,2,3,...,m \tag{48}$$

where the $\hat{x}^k$ is the local minimum at the current k iteration. The penalty parameters are updated via:

$$\gamma_i^{k+1}=\begin{cases}\gamma_i^k & \min(g_i^{k+1},0)\le\varsigma\min(g_i^k,0)\\ \max(\eta\gamma_i^k,k^2) & \min(g_i^{k+1},0)>\varsigma\min(g_i^k,0)\end{cases} \tag{49}$$

where $0<\varsigma<1$ and $\eta>0$; typically, $\varsigma=0.25$ and $\eta=10$ [39].

3.6 Proposed Method

The proposed method for thermo-elastic topology optimization builds upon the Pareto method which is therefore summarized next.

Pareto is a topological sensitivity based method, whose unique feature is that it traces the Pareto-optimal curve governing the optimized quantity of interest φ (such as compliance) and the volume fraction [21].

For a compliance constrained volume minimization problem in Figure 2, the optimization process starts at a volume-fraction of 1 (at the bottom right), and the Pareto-optimal curve is traced in small decrements of volume fractions until the constraints are violated. For detailed description of PareTo, please refer to [21].

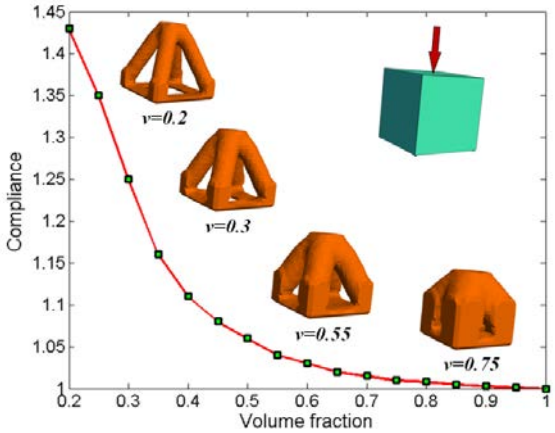

Figure 2: The Pareto-optimal curve and optimal topologies for a 3D structural problem.

3.7 Algorithm

The overall algorithm proceeds as follows:

1. Start the optimization at a volume fraction of 1.0. The 'current volume fraction' v is set to 1.0, and 'volume decrement' Δv, is set to 0.025.
2. Solve the thermo-structural FEA problem in Equation (2) and the stress are extracted at the center of each element by Equation (6).
3. Solve the linear buckling eigen-value problem in Equation (8). The buckling topological sensitivity field is computed at the center of each element and locally smoothened with neighboring elements by either the direct method in Equation (18) or adjoint method in Equation (39).
4. Use augmented Lagrangian formulation to combine the sensitivity fields of the objective function and constraints in Equation(46).
5. Decrement volume fraction by (Δv) and trace the PareTo curve based on the sensitivity of the augmented Lagrangian equation. The compliance is computed over each new topology. If the compliance has converged, then the optimization moves to the next step, else it returns to step 2.
6. The current volume fraction is set to ($v - \Delta v$), and the optimization returns to step-2, until the final volume fraction is reached or the constraints are violated.

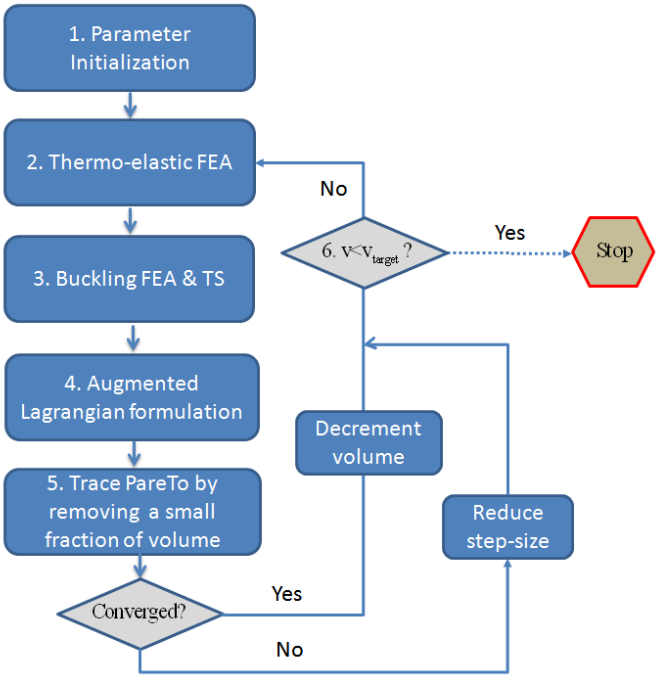

Figure 3: An overview of the algorithm.

4. NUMERICAL EXPERIMENTS

In this Section, we demonstrate the proposed method through numerical experiments. The default parameters are as follows:

- The material is assumed to be steel, i.e., the elastic modulus is $E = 2e11\,Pa$, the Poisson's ratio is $\nu = 0.3$ and the coefficient of thermal expansion is $\alpha = 1.1e-5$.
- The reference temperature is 0^0C, and a thermal load is applied by increasing the temperature uniformly of ΔT.
- Hexahedral elements are used for 3D finite element analysis.

Further, the desired volume fraction is 0.5. In other words, the optimization terminates if the constraints are violated or if the final volume fraction is reached.

4.1 Benchmark example

The first experiment involves the classic thin column structure which was previously studied in [31]. As illustrated in Figure 4, the structure is clamped at bottom and a compressive load of $F = 1e5N$ is applied at the center of the top edge; the structure is also subject to a homogeneous temperature elevation of $\Delta T = 150^0C$.

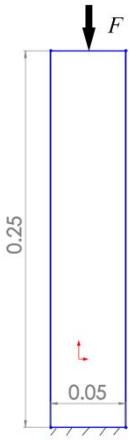

Figure 4: The thin column structure with a thickness of 0.01 (m).

The topology optimization problem considered in this section can be posted as:

$$\begin{aligned} &\underset{\Omega \subset D}{Min} \; |\Omega| \\ &|\Omega| \geq 0.5|D| \\ &J \leq 2.5J_0 \\ &P \geq 0.6P_0 \\ &\text{subject to} \\ &Kd = f_{st} + f_{th} \\ &\Delta T = 150^o C \end{aligned} \tag{50}$$

In words, we search for the optimal design whose final compliance should be no larger than 2.5 times its initial value while the final buckling load factor should be larger than or equal to 60% of its initial value.

In order to test the direct and adjoint methods, we use different numbers of finite elements to mesh the thin column in Figure 4 and compare their computational time. The comparison is shown in Figure 5. It is clear the proposed adjoint method is significantly computational efficient. Since the inverse of the global stiffness matrix (K^{-1}) has to be computed for every single element iteration as illustrated in Equation (28), the computing time of the direct method increase exponentially with the number of finite elements. Therefore, expecting the direct method to finish a large-scale job, normally with over one million DOF, in a reasonably short time is impossible.

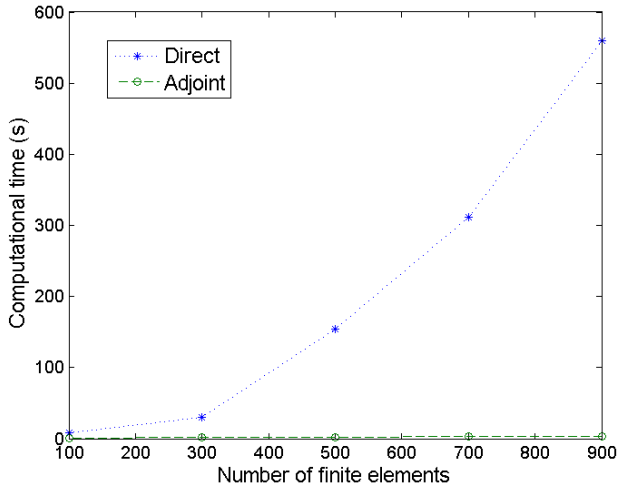

Figure 5: Comparison of computational time between direct and adjoint method.

Due to its simplicity and efficiency, the adjoint method is preferred henceforth. If we use 30,000 elements (i.e., 104,832 DOF) to mesh the design domain, the resulting topologies are shown in Figure 6(a). If the temperature elevation is neglected from Equation (50), i.e. a pure elastic optimization problem is considered, the optimal topology is shown in Figure 6(b). If both the temperature change and the buckling constraint are neglected from Equation (50), i.e. a pure elastic volume-compliance minimization problem is considered, the resulting topology is in Figure 6(c). The impacts of temperature change and buckling constraint on the optimization results are clearly seen. The detailed results are shown in Table 1 where the active constraints are emphasized with a 'box'.

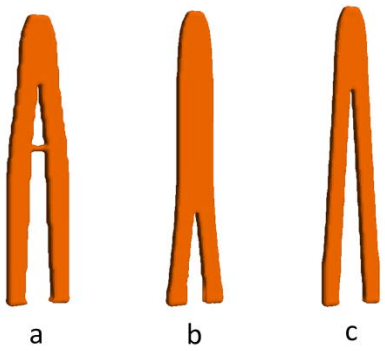

Figure 6: (a) Resulting topology from the adjoint method; (b) buckling-compliance constrained elastic TO; (c) compliance constrained elastic TO.

Table 1: Constraints and results for problem in Figure 6

Topology	Initial Constraints	Final Results	Final volume fraction & time (sec)
Figure 6(b)	$J \leq 2.5J_0$ $P \geq 0.6P_0$ $\Delta T = 200^o C$	$\boxed{J = 2.48J_0}$ $P = 0.91P_0$ $\Delta T = 200^o C$	$V = 0.57$ $T = 197.03$
Figure 6(c)	$J \leq 2.5J_0$ $P \geq 0.6P_0$	$J = 1.48J_0$ $\boxed{P = 0.60P_0}$	$V = 0.59$ $T = 145.68$

Figure 6(d)	$J \le 2.5J_0$	$J = 1.70J_0$	$\boxed{V = 0.5}$ $T = 48.59$

We plot the iteration history and evolving topologies of the adjoint method in Figure 7 and Figure 8, respectively.

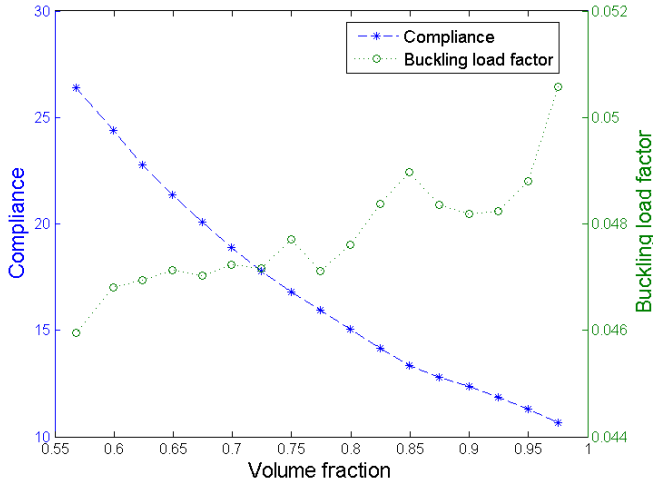

Figure 7: Iteration history of the adjoint approach.

Observe in Figure 7 that with the decrement of volume fraction, the compliance monotonously increases, while the buckling load factor generally decreases.

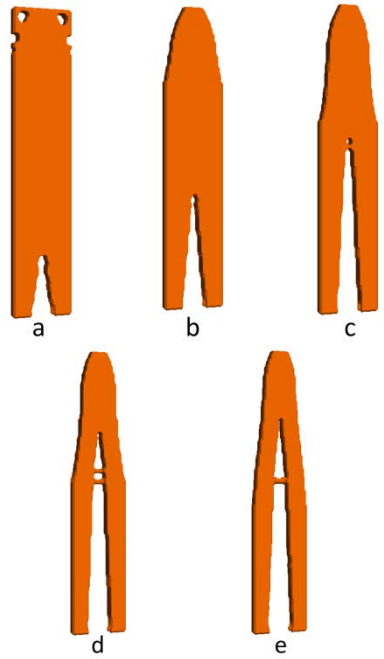

Figure 8: Evolving topologies with different volume fractions: (a) 90%; (b) 80%; (c) 70%; (d) 60%; (e) 57%.

4.2 Industrial application

The purpose of this section is to show the robustness of the proposed adjoint method for a non-trivial application. In particular, a thermo-elastic TO problem over an air plane wing rib structure is studied in this section. The ribs are commonly used in aero-industry to stiffen wing structures. Since the ribs are fastened onto wing skins and are often subject to temperature rise during flight, deduced thermal compressive stress may result in buckling failure.

In this application, we optimize the rib design subject to compliance and buckling constraints with a uniform temperature rise of $\Delta T = 100^o C$. Specifically, we solve the following optimization problem:

$$\begin{aligned} &\underset{\Omega \subset D}{Min} \; |\Omega| \\ &|\Omega| \ge 0.5|D| \\ &J \le 2.0J_0 \\ &P \ge 0.8P_0 \\ &\text{subject to} \\ &Kd = f_{st} + f_{th} \\ &\Delta T = 100^o C \end{aligned} \tag{51}$$

As shown in Figure 9, the rib is fixed at top surface and a vertical force of $P = 1e8(N/\mathrm{m}^2)$ is applied upward at the bottom surface. The outer surface and two inside holes are retained during TO. For FEA, 15,028 hexahedral elements are used to discretize the design domain, resulting in 70,767 DOF.

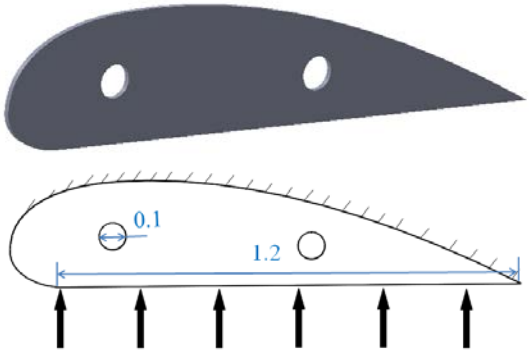

Figure 9: 3D rib structure (above) and applied FEA boundary conditions (bottom)

The resulting topology is shown in Figure 10 and the results are detailed in Table 2.

Figure 10: Final optimal design for the thermally restrained rib structure

Table 2: Constraints and results for problem in Figure 10

Topology	Initial Constraints	Final Results	Final volume fraction & time (s)
Figure 6(a)	$J \le 2.0J_0$ $P \ge 0.8P_0$ $\Delta T = 100^o C$	$J = 2.0J_0$ $\boxed{P = 0.90P_0}$ $\Delta T = 100^o C$	$V = 0.64$ $T = 161.85s$

5. CONCLUSIONS

The main contribution of the paper is a new method for buckling constrained thermo-elastic topology optimization algorithm. Two different formulations were presented and

compared. Both formulations exploit the concept of topological sensitivity; thus material parameterization is not required.

As the numerical experiments reveal, the impact of temperature variations on the final topologies can be significant for certain problems. Future work will focus on non-linear buckling analysis of large-deformation.

Acknowledgements

The authors would like to thank the support of National Science Foundation through grants CMMI-1232508 and CMMI-1161474.

REFERENCES

[1] H. A. Eschenauer and N. Olhoff, "Topology optimization of continuum structures: A review," *Applied Mechanics Review*, vol. 54, no. 4, pp. 331–389, 2001.

[2] G. I. N. Rozvany, "A critical review of established methods of structural topology optimization," *Structural and Multidisciplinary Optimization*, vol. 37, no. 3, pp. 217–237, 2009.

[3] E. Kesseler, "Multidisciplinary design analysis and multi-objective optimisation applied to aircraft wing," *WSEAS transactions on systems and Control and Cybernetics*, vol. 1, no. 2, p. 221 227, 2006.

[4] J. J. Alonso, "Aircraft design optimization," *Mathematics and Computers in Simulation*, vol. 79, no. 6, pp. 1948–1958, 2009.

[5] V. H. Coverstone-Carroll, "Optimal multi-objective low-thrust spacecraft trajectories," *Comput. Methods Appl. Mech. Eng.*, vol. 186, pp. 387–402, 2000.

[6] L. Wang, "Automobile body reinforcement by finite element optimization," *Finite Elements in Analysis and Design*, vol. 40, no. 8, pp. 879–893, 2004.

[7] L. Harzheim, "A review of optimization of cast parts using topology optimization II-Topology optimization with manufacturing constraints," *Structural and Multidisciplinary Optimization*, vol. 31, no. 5, pp. 388–299, 2006.

[8] G. K. Ananthasuresh, S. Kota, and Y. Gianchandani, "A methodical approach to the design of compliant micromechanisms," in *Solid State Sensor and Actuator Workshop*, 1994, pp. 189–192.

[9] S. Nishiwaki, "Topology Optimization of Compliant Mechanisms using the Homogenization Method," *International Journal for Numerical Methods in Engineering*, vol. 42, pp. 535–559, 1998.

[10] T. E. Bruns and D. A. Tortorelli, "Topology optimization of non-linear elastic structures and compliant mechanisms," *Computer Methods in Applied Mechanics and Engineering*, vol. 190, no. 26–27, pp. 3443–3459, 2001.

[11] Z. Luo, "Compliant mechanism design using multi-objective topology optimization scheme of continuum structures," *Structural and Multidisciplinary Optimization*, vol. 30, pp. 142–154, 2005.

[12] R. D. Cook, D. S. Malkus, M. E. Plesha, and R. Witt, *Concepts and Applications of Finite Element Analysis*, 4th ed. John Wiley & Sons, 2002.

[13] M. Zhou, "Difficulties in truss topology optimization with stress and local buckling constraints," *Structural Optimization*, vol. 11, no. 2, pp. 134–136, 1996.

[14] W. Achtziger, "Local stability of trusses in the context of topology optimization part I: exact modelling," *Structural Optimization*, vol. 17, no. 4, pp. 235–246, 1999.

[15] X. Guo, G. Cheng, and K. Yamazaki, "A new approach for the solution of singular optima in truss topology optimization with stress and local buckling constraints," *Structural Optimization*, vol. 22, no. 5, pp. 364–373, 2001.

[16] K. Mela, "Resolving issues with member buckling in truss topology optimization using a mixed variable approach," *Struct Multidisc Optim*, vol. 50, no. 6, pp. 1037–1049, 2014.

[17] O. Sigmund, "A 99 line topology optimization code written in Matlab," *Structural and Multidisciplinary Optimization*, vol. 21, no. 2, pp. 120–127, 2001.

[18] X. Guo and G. D. Cheng, "Epsilon-continuation approach for truss topology optimization," *Acta Mechanica Sinica*, vol. 20, no. 5, pp. 526–533, 2004.

[19] C. Le, "Developments in topology and shape optimization," PhD thesis, University of Illinois at Urbana-Champaign, Urbana-Champaign, 2010.

[20] S. Wang, E. D. Sturler, and G. Paulino, "Large-scale topology optimization using preconditioned Krylov subspace methods with recycling," *International Journal for Numerical Methods in Engineering*, vol. 69, no. 12, pp. 2441–2468, 2007.

[21] K. Suresh, "Efficient Generation of Large-Scale Pareto-Optimal Topologies," *Structural and Multidisciplinary Optimization*, vol. 47, no. 1, pp. 49–61, 2013.

[22] M. M. Neves, H. Rodrigues, and J. M. Guedes, "Generalized topology design of structures with a buckling load criterion," *Structural Optimization*, vol. 10, no. 2, pp. 71–78, Oct. 1995.

[23] M. Bendsøe and O. Sigmund, *Topology Optimization: Theory, Methods and Application*, 2nd ed. Springer, 2003.

[24] M. Zhou, "Topology optimization for shell structures with linear buckling responses," presented at the WCCM VI, Beijing, China, 2004.

[25] E. Lindgaard and J. Dahl, "On compliance and buckling objective functions in topology optimization of snap-through problems," *Struct Multidisc Optim*, vol. 47, no. 3, pp. 409–421, 2013.

[26] X. Gao and H. Ma, "Topology optimization of continuum structures under buckling constraints," *Computers & Structures*, vol. 157, pp. 142–152, 2015.

[27] D. J. Munk, G. A. Vio, and G. P. Steven, "Topology and shape optimization methods using evolutionary algorithms: a review," *Struct Multidisc Optim*, pp. 1–19, May 2015.

[28] X. Huang and Y. M. Xie, "A new look at ESO and BESO optimization methods," *Structural and Multidisciplinary Optimization*, vol. 35, no. 1, pp. 89–92, 2008.

[29] J. H. Rong, Y. M. Xie, and X. Y. Yang, "An improved method for evolutionary structural optimisation against buckling," vol. 79, no. 3, pp. 253–263, 2001.

[30] N. P. van Dijk, K. Maute, M. Langelaar, and F. van Keulen, “Level-set methods for structural topology optimization: a review,” *Structural and Multidisciplinary Optimization*, vol. 48, no. 3, pp. 437–472, 2013.

[31] X. Bian, P. Yadav, and K. Suresh, “Assembly-Free Buckling Analysis for Topology Optimization,” presented at the ASME-IDETC Conference, Boston, MA, 2015.

[32] S. Osher, “Level-set methods for optimization problems involving geometry and constraints: frequencies of a twodensity inhomogeneous drum,” *Journal of Computational Physics*, vol. 171, pp. 272–288, 2001.

[33] J. Deaton and R. V. Grandhi, “Topology Optimization of Thermal Structures with Stress Constraints,” presented at the 54th AIAA/ASME/ASCE/ASC Structures, Structural Dynamics, and Materials Conference, Boston, MA, 2013.

[34] R. B. Hetnarski, J. Ignaczak, N. Noda, N. Sumi, and Y. Tanigawa, *Theory of Elasticity and Thermal Stresses: Explanations, Problems and Solutions*. Springer, 2013.

[35] S. J. van den Boom, “Topology Optimisation Including Buckling Analysis,” Delft University of Technology, Delft, 2014.

[36] M. P. Bendsøe, “Optimal shape design as a material distribution problem,” *Structural Optimization*, vol. 1, no. 193–202, 1989.

[37] P. Yadav and K. Suresh, “Large Scale Finite Element Analysis Via Assembly-Free Deflated Conjugate Gradient,” *J. Comput. Inf. Sci. Eng*, vol. 14, no. 4, pp. 41008-1-9, 2014.

[38] A. M. Mirzendehdel and K. Suresh, “A Pareto-Optimal Approach to Multimaterial Topology Optimization,” *Journal of Mechanical Design*, vol. 137, no. 10, 2015.

[39] J. Nocedal and S. Wright, *Numerical Optimization*. Springer, 1999.